B8 Project: X-ray Single-Photon Energy-Dispersive Spectroscopy (XSPEDS)

Candidate Number: 1259500
Project number: B8_03
Supervisor: S. M. Vinko

1 Abstract

We use data from pairing a Bragg Spectroscopy setup with a CCD detector. Photons can be found and counted on the image, and Bragg's law allows us to use spatial position of those photons on the image to determine their energy. Using this information we can plot a spectrum of throughput of photons against energy.

2 Introduction

2.1 Experimental setup and data

For this project we used data from an experiment diagnosing a plasma using a flat-crystal Bragg spectrometer, diffracting X-rays before they are recorded at a CCD camera.
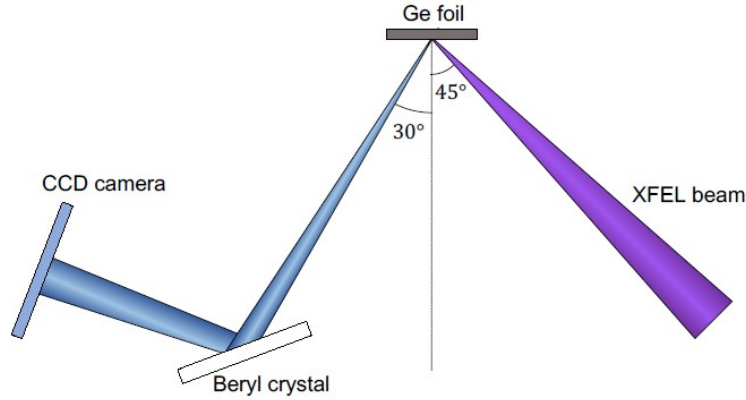

Figure 1: An X-ray free electron laser beam impinges on a Ge foil, and the light produced from this is diffracted by a beryl crystal before reaching the CCD camera

For more details on the experiment setup see [1].

2.2 Geometry and Bragg's Law

In order to create a spectrum of energy against photon count, we must be able to find the energy of a photon based on its position on the CCD. We can first start with Bragg's Law, which says that for a wave of wavelength λ incident on a crystal with grating constant d, its glancing angle for constructive interference, θ will be related by:

$$n\lambda = 2d \sin \theta \tag{1}$$

where n is the diffraction order.

Relating wavelength to photon energy allows us to relate glancing angle to photon energy:

$$n \times \frac{hc}{E} = 2d \sin \theta \tag{2}$$

As waves of the same wavelength (and therefore same energy) interfere constructively at the same glancing angles, photons corresponding to the spectral lines of our sample will form bright, curved fringes on our CCD image. Having the same glancing angle also means that these photons will form a cone, and at the CCD the fringe will be a conic section.

1

2.3   CCD Operation and Single Photon Counting

In the dark, a CCD detector produces still produces signal, due to the electronics, thermal electrons in the chip known as 'dark current', and shot noise. These sources of noise can be approximated as a Gaussianly distributed set of random numbers, as seen in figure 7. When a photon is incident on the CCD, it will generate some number of electron-hole pairs proportional to the photon energy. For example in silicon on average an X-ray photon will create electron hole pairs at a rate of 3.65eV per pair [2]. This translates to an increase in the ADU value of a pixel, with a constant of proportionality known as the gain, so genrally speaking,

$$\text{ADU value} = \text{background} + \text{gain} \times \text{electron hole pairs} \tag{3}$$

In practice, there are fluctuations in the average energy required to produce an electron-hole pair, and these fluctuations are summarized in a number known as the Fano factor. In summary, additional ADU value above background should be directly proportional to the energy of an incident photon.

When a photon is incident on the CCD, it will liberate electrons, which in turn increase the ADU value of that pixel, and due to charge spread it may also increase the ADU value of neighbouring pixels. By looking for local peaks in ADU values that are above the pedestal distribution, we are able to pinpoint and count photons on the CCD.

3   Methods and Analysis

3.1   Identification and curve-fitting of Spectral Lines

In the data we used there were two spectral lines, at 1188.0 eV and at 1218.5 eV, as well as other photons produced at a distribution of energies known as the bremsstrahlung. For the purpose of identifying and fitting the two spectral lines, we added multiple frames together to get a better signal-to-noise ratio. As there are a higher density of photons incident at the energies of the two spectral lines, there is a higher average ADU value in the regions corresponding to those lines. By applying a Gaussian filter (see 2), local maxima in ADU values, which correspond to incident photons, will merge together to form a distinct peak, which we can then identify as being part of that line.

We found this process to be relatively robust but sometimes gave anomalous points that clearly don't lie on the line, which we then have to remove 4.

Once we have found enough points corresponding to the two spectral lines, we used least-squares curve fitting to find parameters defining the geometry of the experiment. We can then calculate the energies corresponding to all the different pixels, and create a map of energies corresponding to every location on the CCD image 5.

3.2   Creating a spectrum by averaging ADU values

Now that we can calculate the energies of photons incident on any pixels we can make our first attempt at a spectrum. The simplest way of doing this is by splitting up the image into equally spaced bins in energy, and finding the average of the ADU values of all the pixels in each bin 6. The advantage of this method is that it doesn't rely on having an arbitrary threshold the way single photon counting does, and it doesn't need to distinguish between single and multi-photon events the same way single-photon counting does. On average, photons of the same energy should contribute the same amount to the average ADU value of some energy bin, so if we know the gain and average background then this should be reliable. Because most of the pixels are background, it becomes very important to know the average background with great precision, which we can't have just by looking at the pedestal. We also don't know the gain.

3.3   Creating a spectrum from single-photon counting

Another way of creating a spectrum is by single-photon counting. To perform single-photon counting, we first defined a threshold by calculating the minimum ADU value on the image plus twice the distance between the minimum and the peak of the pedestal 7. This way we can be confident that all pixels that are above this value lie outside the pedestal. Then, to count photons we look for pixels with ADU values above the threshold that are also higher than the 8 neighbouring pixels. Once we have identified all the photons, and their energies based on their location on the image, we can put count the number of photons in each
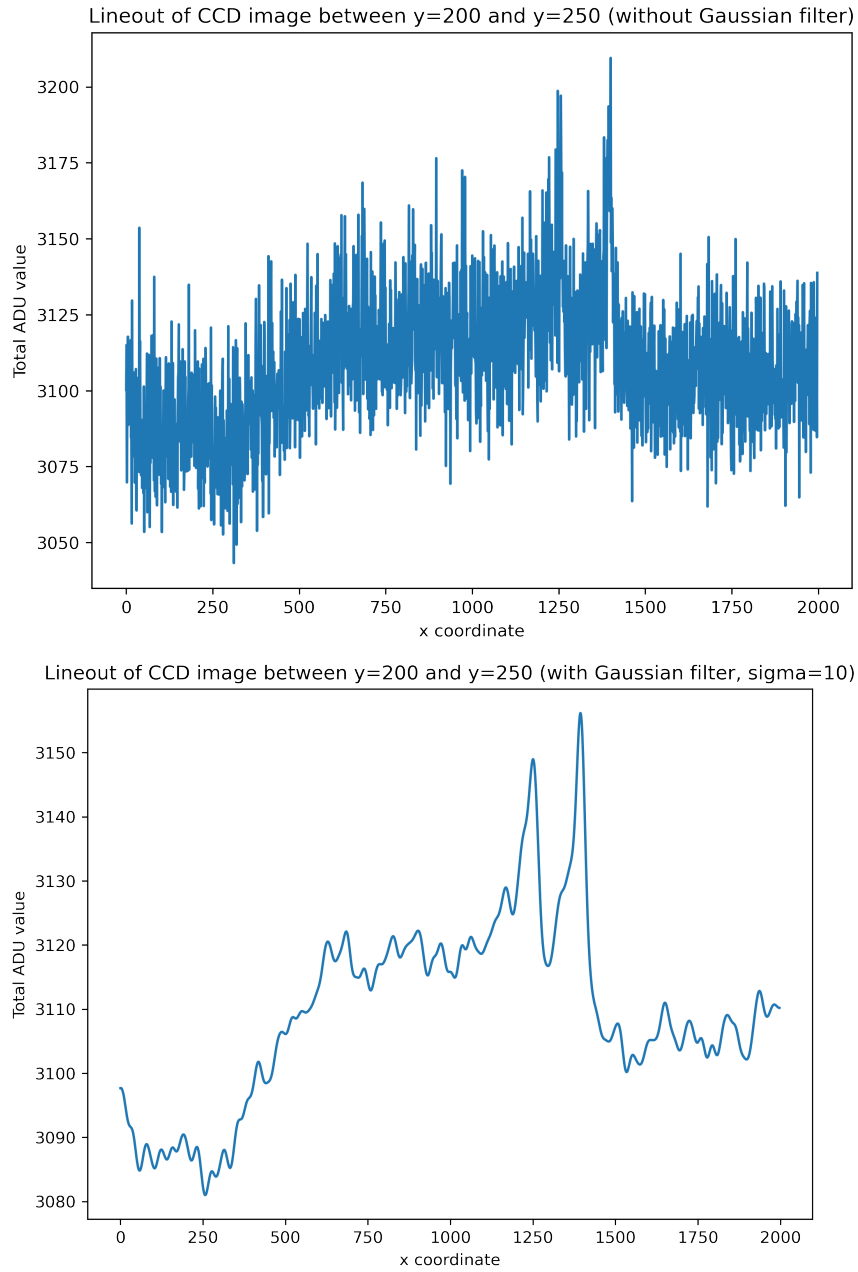
Figure 2: Lineouts of a small slice of the image between y=200 and y=250 taken before and after applying a Gaussian filter. The Gaussian filter makes it easier two identify the x-coordinates of the two peaks that correspond to the spectral lines.
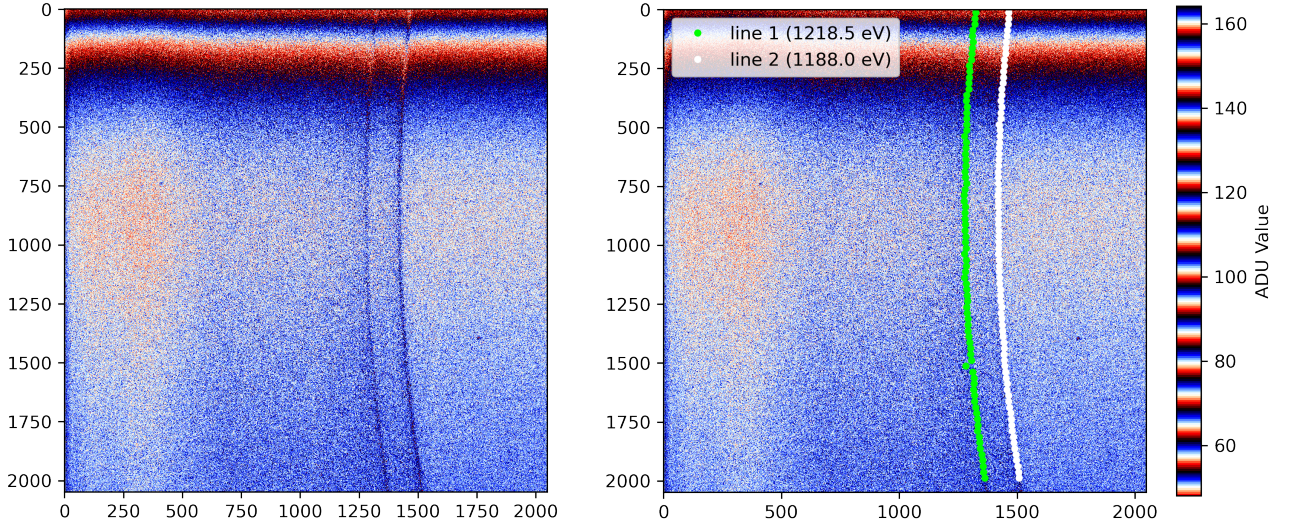
Figure 3: Using the method outlined above we were able to identify the two lines on the raw image (left), with points on the two spectral lines indicated by the white and green dots (right). Colorbar is the same for both images and meant to make small differences in ADU value more visible, which makes the two lines easier to see.
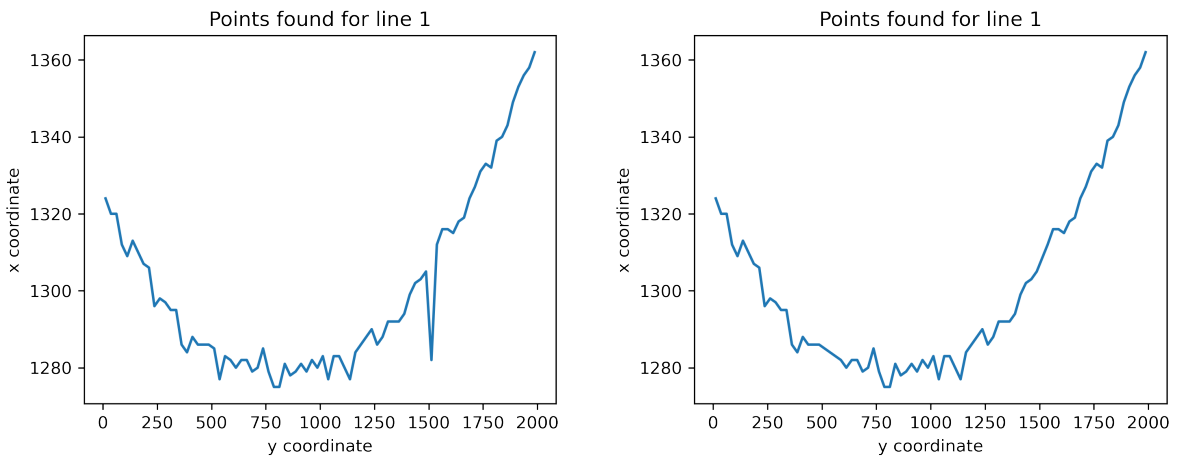

Figure 4: Our method of finding points on the spectral lines is not 100% robust and sometimes, due to noise, creates outliers which need to be removed. Left: Points found for line 1, before outlier removed. Right: Points found for line 1, after outlier removed.
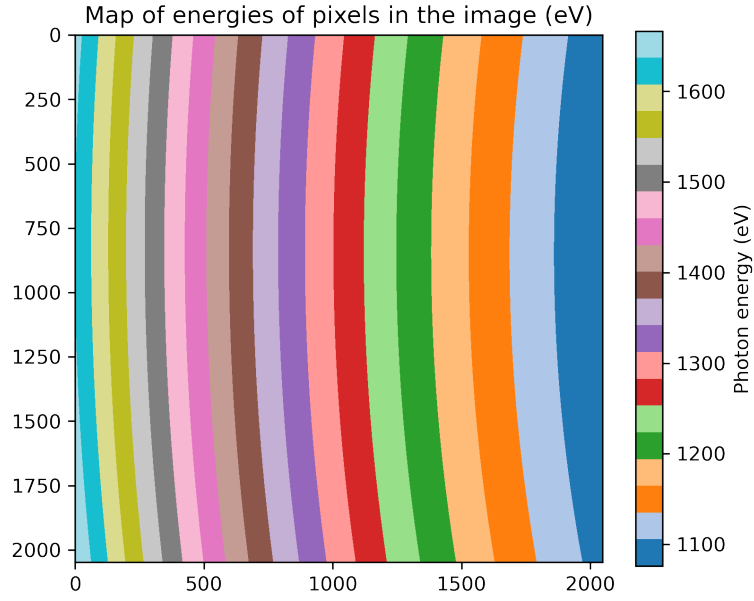
Figure 5: Map of energies for each pixel. The discrete colour scheme shows how the width, curvature, and area of each energy bin varies.
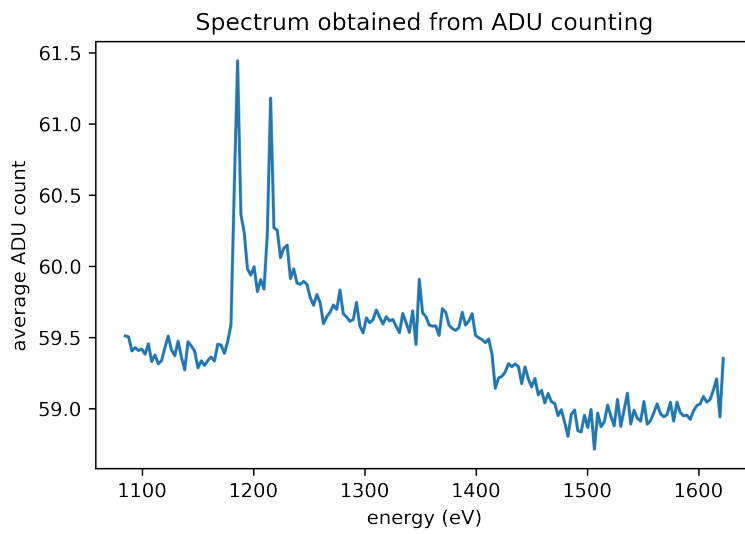

Figure 6: Spectrum which shows average ADU value for pixels in each energy bin.

energy bin to create a spectrum (figure 8). The disadvantage of this method is that due the Fano factor, there will be some photon events with ADU values below this threshold, which will lead us to under-count the number of photon events. This method is also not robust in the case where there is a high density of photon events and a large proportion of multi-photon events, because in the case of overlapping photon events, there may only be one pixel with the peak ADU value, rather than two or more.
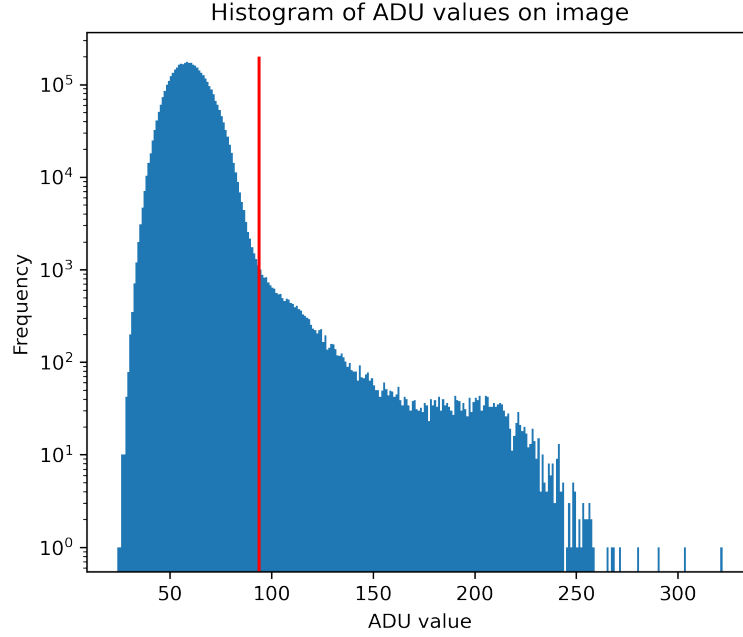

Figure 7: Histogram of ADU values of the image we are analysing. The red line marks the threshold we chose for single-photon counting. The part of the histogram to the left of this red line has 'pedestal' shape characteristic of a the background on our CCD.
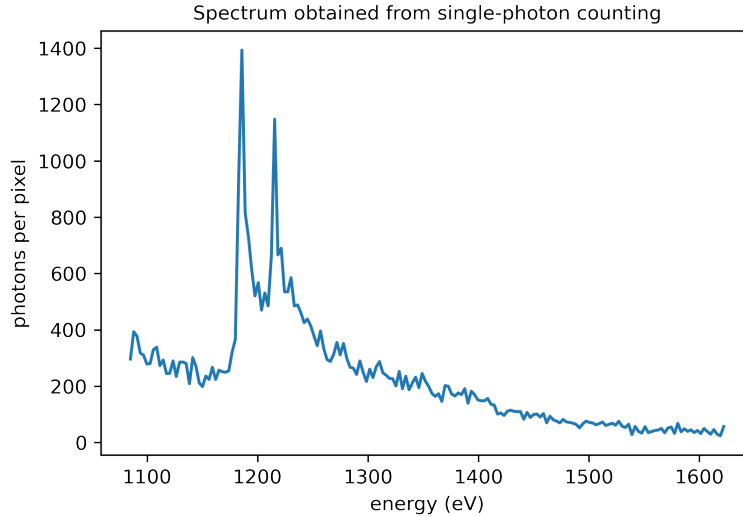

Figure 8: Spectrum which the number of photon events found per pixel in each bin, using our single-photon counting algorithm.

3.4 Combining the two methods

By combining these two methods, we can in theory check both whether our answers are reasonable, and and get a better spectrum than by using either method. By plotting average ADU value for each bin against number of photons found per pixel of each bin times the photon energy of that bin, we found a clear linear relationship 9. As expected, the regions with a very high average ADU value do not follow this linear relationship because this is where there is a large proportion of multi-photon events, where

our single-photon counting algorithm cannot reliably distinguish between single- and multi-photon events. Looking at the intercept gives us the average background value, which is not far off the center of the pedestal we find from the histogram of ADU values 7. The gradient gives us a value for ADU per photon event per eV which is much higher than we expect: 5ADU per eV per photon event, which means for a 1000eV photon we detect, there's an additional 5000ADU for that bin. As the pixel with the greatest ADU value in this image is around 300ADU, this suggests that we are severely under-counting the number of photons in the image by a factor of at least 10. That being said, the fact that we have a straight line relationship between density of photon events and average ADU value suggests that we are detecting a constant proportion of the photon events on the CCD, which means the spectrum is affected only by some constant of proportionality.
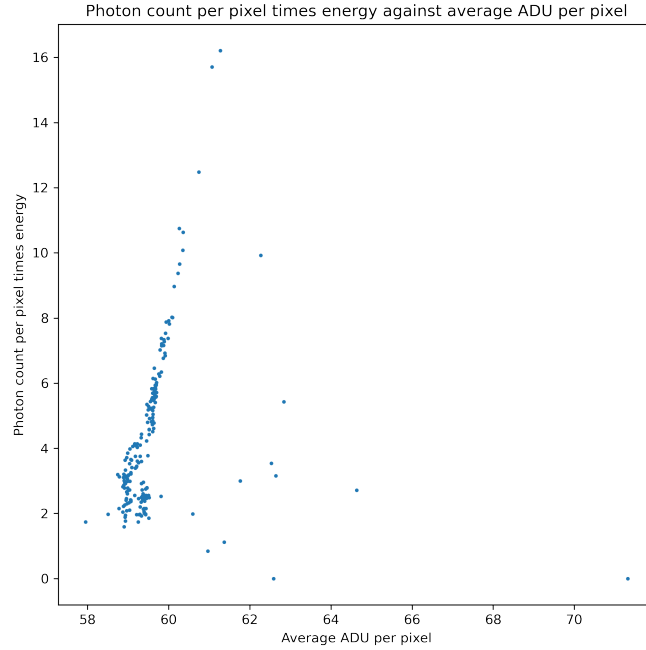

Figure 9: There is a clear linear relationship between the two methods of creating a spectrum, with the outliers tending to be at higher average ADU values, which is where there are more multi-photon events.

3.5 Uncertainties

For each bin, the number of incident photons and therefore the number of photons detected is a Poisson process, i.e. there is a constant average flux of photons into each region, and incident photon events are independent of each other. For a Poisson process, the standard deviation is the square root of the number of events. For this final spectrum, we took the uncertainty in photon count to be one standard deviation, and converted that into a percentage uncertainty before normalising the spectrum.

3.6 Normalization

So far throughout this we have normalized the spectrum to the number of photon events per pixel found, because it has been convenient for our analysis. This, however doesn't exactly reflect the throughput of photons coming from the source we are trying to diagnose. Let's say that the number of photons being produced by the source at an energy between E and $E + dE$ is given by $\epsilon(E)dE$. This will be related to the number of photons reflected off the crystal per unit solid angle $f(\theta)$ by:

$$f(\theta)\sin\theta d\theta d\phi = \epsilon(E)dE$$

assuming photons are emitted uniformly at every angle ϕ gives us,

$$2\pi f(\theta)\sin\theta d\theta = \epsilon(E)dE$$

where $d\theta$ can be calculated by relating energy and θ from Braggs law (equation 2). In practice of course photons aren't emitted uniformy at every angle ϕ, but as long as we are looking at a relatively small amount of the total solid angle from where the photons are reflected off the crystal, this assumption should work for normalising our spectrum. Given the parameters we found by curve fitting the spectral lines, we can calculate the total solid angle covered by the pixels in each energy bin, and given that we know the number of incident photons for each bin, we should be able to calculate $f(\theta)$ and re-normalise the spectrum to give us $\epsilon(E)$, within a constant of proportionality (see figure 10).
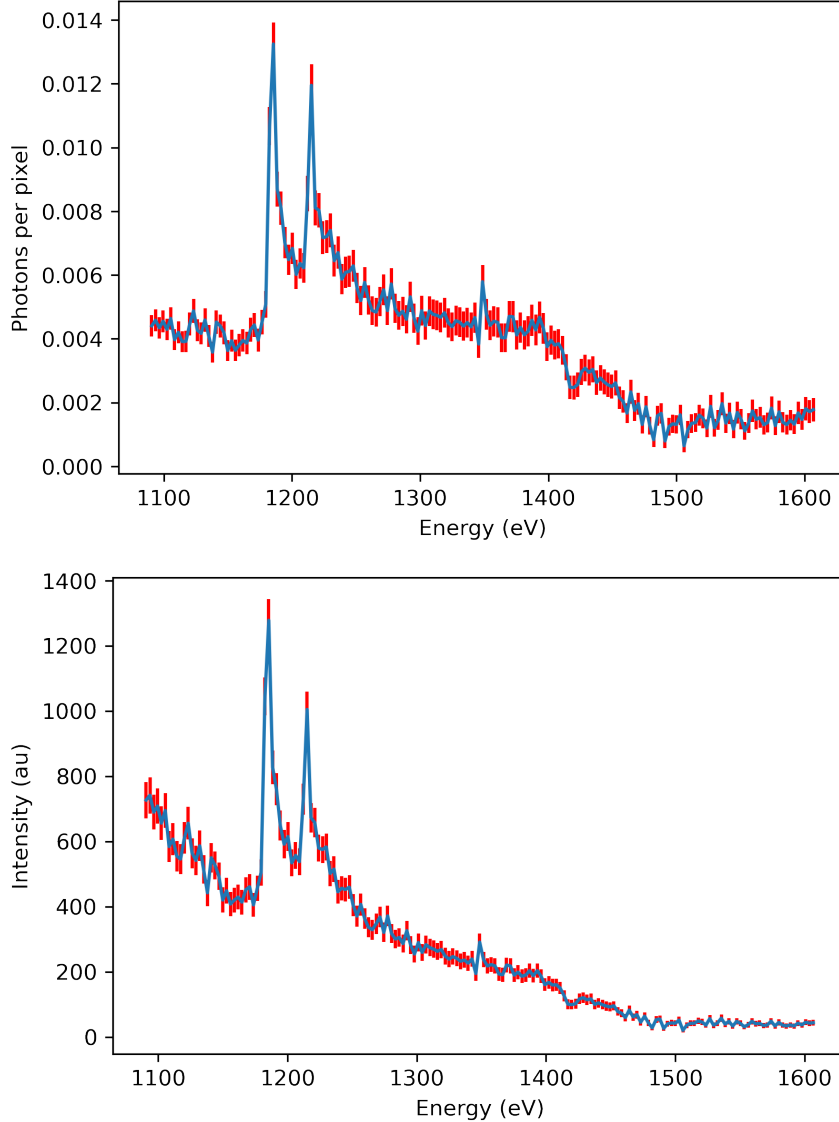

Figure 10: Spectrum we find, top: normalised to per pixel in each bin, bottom: converted to total intensity for each bin

4 Conclusions

The method we have outlined above for extracting a spectrum from a CCD image, while relatively robust, still relies on many assumptions. A key issue is that the relationship shown in figure 9 is more complicated than a straight line relationship, with a large number of values that are clustered just off the best fit straight line, in a region with lower ADU and lower density of photon events. This could indicate that our single photon counting algorithm is not robust in the regime of a low density of photon events, possibly due to an increase in the number of 'false positive' photons, i.e. local maxima in ADU value simply caused by noise. This would make sense, as in the middle regime, the regime where photon events are not sparse but not overlapping, a straight line works very well, which may be because those 'false' photon events caused by noise are form a smaller proportion of the photon events we find.

References

[1] Gabriel Pérez-Callejo, Sam M. Vinko, Shenyuan Ren, Ryan Royle, Oliver Humphries, Thomas R. Preston, Bruce A. Hammel, Hyun-Kyung Chung, Tomas Burian, Vojtěch Vozda, Ming-Fu Lin, Tim Brandt van Driel, and Justin S. Wark. X-ray spectroscopic studies of a solid-density germanium plasma created by a free electron laser. *Applied Sciences*, 10(22), 2020.

[2] Sam Vinko. B8 lecture 2, 2021. Lectures on B8 Project.